Oligothiophenes End-Capped by Nitriles. Preparation and Crystal Structures of α,ω-Dicyanooligothiophenes $NC(C_4H_2S)_nCN$ ($n = 3-6$)

T. M. Barclay,[1a] A. W. Cordes,*[,1a] C. D. MacKinnon,[1b] R. T. Oakley,*[,1b] and R. W. Reed[1b]

Department of Chemistry and Biochemistry, University of Arkansas, Fayetteville, Arkansas 72701, and Department of Chemistry and Biochemistry, University of Guelph, Guelph, Ontario N1G 2W1, Canada

Received October 23, 1996[⊗]

The synthesis of dicyanooligothiophenes $NC(C_4H_2S)_nCN$ ($n = 3-6$) is reported. For $n = 3$, 4, and 5 the dinitriles are generated by treatment of the corresponding dibromo compounds with copper(I) cyanide in quinoline. For $n = 6$ the preparation involves the Ni-catalyzed coupling of 5-bromo-2,2′:5′,2″-terthiophene-5″-carbonitrile. The structures of all four dicyano derivatives have been determined by X-ray crystallography. For $n = 3$, the space group is monoclinic $C2/c$, with $a = 18.363(7)$, $b = 11.8356(9)$, $c = 30.666(4)$ Å, $\beta = 102.15(2)°$, $V = 6515(3)$ Å^3, $Z = 20$. For $n = 4$ the space group is triclinic $P\bar{1}$, $a = 7.3254(9)$, $b = 7.8658(6)$, $c = 8.1813(8)$ Å, $\alpha = 64.706(8)$, $\beta = 76.059(8)$, $\gamma = 76.692(8)°$, $V = 409.29(7)$ Å^3, $Z = 1$. For $n = 5$ the space group is monoclinic $C2/c$, with $a = 13.633(4)$, $b = 11.706(5)$, $c = 37.073(8)$ Å, $\beta = 90.22(2)°$, $V = 5929(3)$ Å^3, $Z = 12$. For $n = 6$, the space group is monoclinic $P2_1/a$, with $a = 13.8962(14)$, $b = 5.9100(16)$, $c = 14.0798(16)$ Å, $\beta = 98.446(4)°$, $V = 1143.8(4)$ Å^3, $Z = 2$. In all four structures the molecules are approximately planar, with all-trans thiophene rings. The oligomers are linked into ribbonlike arrays by intermolecular CN- - -H contacts. For $n = 3$, 4, and 5 these ribbons are stacked in approximately coplanar layers (π-stacks). For $n = 6$ the ribbons are packed in a herringbone motif very similar to that observed in $H(C_4H_2S)_6H$ (α-6T). The UV−visible spectra of $NC(C_4H_2S)_nCN$ ($n = 2-6$) have been recorded, and shifts in the $\pi-\pi^*$ excitation energies of these compounds relative to those found in other α,ω-disubstituted oligothiophenes are interpreted in the light of MNDO calculations. Extended Hückel band structure calculations on $NC(C_4H_2S)_nCN$ ($n = 4$ and 6) indicate substantial intermolecular interactions; both structures have well-developed 2-dimensional electronic structures.

Introduction

Oligothiophenes have been investigated for potential use in a variety of devices. These include nonlinear optics,[2] Schottky diodes,[3] LEDs,[4] and thin-film field effect transistors (FETs).[5] The applications of oligothiophenes in thin-film transistors is especially attractive, and numerous efforts toward improving the two important characteristics, on−off ratio and mobility, of the films are underway in different laboratories. Within this context the first[5a] and most heavily studied oligomer is α-sexithiophene (H_2T_6). Recent efforts on improvement include the use of highly purified oligomer,[6] high-temperature film deposition,[7] and single crystals,[8] leading to better ordering of molecules in the film and therefore improved transistor performance. Chemical modifications have been proposed as well. The use of alkyl groups on the α,ω-positions of oligothiophenes R_2T_n has also been investigated. This has the 2-fold benefit of blocking these positions to further reactions, e.g., oxidation and polymerization, and of introducing ordering in the crystal. Very high mobility has been demonstrated when the terminal hydrogens of sexithiophene were replaced by *n*-hexyl groups.[9] Less success has been met with methyl,[5e,10] ethyl,[5d] and hexylthio[11] end-groups.

[⊗] Abstract published in *Advance ACS Abstracts,* March 15, 1997.

(1) (a) University of Arkansas. (b) University of Guelph.

(2) (a) Zhao, M.-T.; Singh, B. P.; Prasad, P. N. *J. Chem. Phys.* **1988**, *89*, 5535. (b) Thienpont, H.; Rikken, G. L. J. A.; Meijer, E. W.; ten Hoeve, W.; Wynberg, H. *Phys. Rev. Lett.* **1990**, *65*, 2141. (c) Wada, T.; Wang, L.; Fichou, D.; Higuchi, H.; Ojima, J.; Sasabe, H. *Mol. Cryst. Liq. Cryst. Sci. Technol. Sect. A* **1994**, *255*, 149.

(3) (a) Fichou, D.; Horowitz, G.; Nishikitani, Y.; Garnier, F. *Chemtronics* **1988**, *3*, 176. (b) Fichou, D.; Horowitz, G.; Nishikitani, Y.; Roncali, J.; Garnier, F. *Synth. Met.* **1989**, *28*, C729. (c) de Leeuw, D. M.; Lous, E. J. *Synth. Met.* **1994**, *65*, 45.

(4) (a) Geiger, F.; Stoldt, M.; Schweizer, H.; Bauerle, P.; Umbach, E. *Adv. Mater.* **1993**, *5*, 922. (b) Uchiyama, K.; Akimichi, H.; Hotta, S.; Noge, H.; Sakaki, H. *Mater. Res. Soc. Symp. Proc.* **1994**, *328*, 389.

(5) (a) Horowitz, G.; Fichou, D.; Peng, X.; Xu, Z.; Garnier, F. *Solid State Commun.* **1989**, *72*, 381. (b) Horowitz, G.; Peng, X.; Fichou, D.; Garnier, F. *J. Appl. Phys.* **1990**, *67*, 528. (c) Paloheimo, J.; Kuivalainen, P.; Stubb, H.; Vuorimaa, E.; Yli-Lahti, P. *Appl. Phys. Lett.* **1990**, *56*, 1157. (d) Akimichi, H.; Waragai, K.; Hotta, S.; Kano, H.; Sakaki, H. *Appl. Phys. Lett.* **1991**, *58*, 1500. (e) Waragai, K.; Akimichi, H.; Hotta, S.; Kano, H.; Sakaki, H. *Synth. Met.*, **1993**, *55−57*, 4053. (f) Garnier, F.; Hajlaoui, R.; Yassar, A.; Srivastava, P. *Science* **1994**, *265*, 1684. (g) Dodabalapur, A.; Katz, H. E.; Torsi, L.; Haddon, R. C. *Science* **1995**, *269*, 1560.

(6) Katz, H. E.; Torsi, L.; Dodabalapur, A. *Chem. Mater.* **1995**, *7*, 2235.

(7) Servet, B.; Horowitz, G.; Ries, S.; Lagorsse, O.; Alnot, P.; Yassar, A.; Deloffre, F.; Srivastava, P.; Hajlaoui, R.; Lang, P.; Garnier, F. *Chem. Mater.* **1994**, *6*, 1809.

(8) Horowitz, G.; Garnier, F.; Yassar, A.; Hajlaoui, R.; Kouki, F. *Adv. Mater.* **1996**, *8*, 52.

(9) Garnier, F.; Yassar, A.; Hajlaoui, R.; Horowitz, G.; Deloffre, F.; Servet, B.; Ries, S.; Alnot, P. *J. Am. Chem. Soc.* **1993**, *115*, 8716.

(10) Waragai, K.; Akimichi, H.; Hotta, S.; Kano, H.; Sakaki, H. *Phys. Rev. B* **1995**, *52*, 1786.

S0897-4756(96)00545-5 CCC: $14.00

Despite the interest in these compounds, very few examples have been fully structurally characterized. Although there have been X-ray powder studies performed on the higher order oligothiophenes (quater-, quinque-, and sexithiophene),[12] growing single crystals of these is difficult due to their lack of solubility. Of the unsubstituted α-oligothiophenes, only bithiophene[13] and terthiophene[14] single crystals have been grown from solution. There have been two recently published reports of the structure of sexithiophene, one using crystals grown from a melt,[15] the other crystals obtained by sublimation.[16] The two structures are very similar, with chains of molecules consisting of all-trans coplanar thiophene rings packed in a herringbone motif. The single-crystal structure of octithiophene from sublimed crystals has also recently been solved.[17] In the case of α,ω-disubstituted oligothiophenes with $n > 2$ only dimethylquaterthiophene[18] and bis(triisopropylsilyl)-sexithiophene[19] have, to our knowledge, been fully characterized.

This dearth of structural information has prompted us to investigate systematically how end-groups can be used to influence and perhaps control the solid-state structures of oligothiophenes. In this paper we describe the synthesis and crystal structures of the α,ω-dicyano-substituted oligothiophenes $(CN)_2T_n$ ($n = 3-6$). We chose the nitrile group as substituent because we believed it to be small enough to allow close intermolecular contacts in the solid state while, at the same time, influencing the ordering of oligothiophene chains through the development of intermolecular CN- - -H interactions, e.g., **1**. In the parlance of crystal engineering, we wished to investigate the use of such interactions as supramolecular synthons.[20]

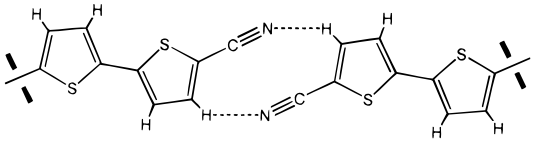

1

Results and Discussion

Synthesis. 2,5-Dicyanothiophene $(CN)_2T$[21] and 2,2′-bithiophene-5,5′-dicarbonitrile $(CN)_2T_2$[22] are known compounds. The former is prepared by treatment of the corresponding dibromothiophene with copper(I) cyanide, while the latter is usually prepared by the reductive coupling of 2-bromo-5-cyanothiophene with copper. There is a recent report of the in situ electrochemical generation of $(CN)_2T_6$, but characterization of the product was limited.[23] Our synthetic work on the series $(CN)_2T_n$ ($n = 3-6$) builds off the general strategies developed for $n = 1$ and 2.

Scheme 1

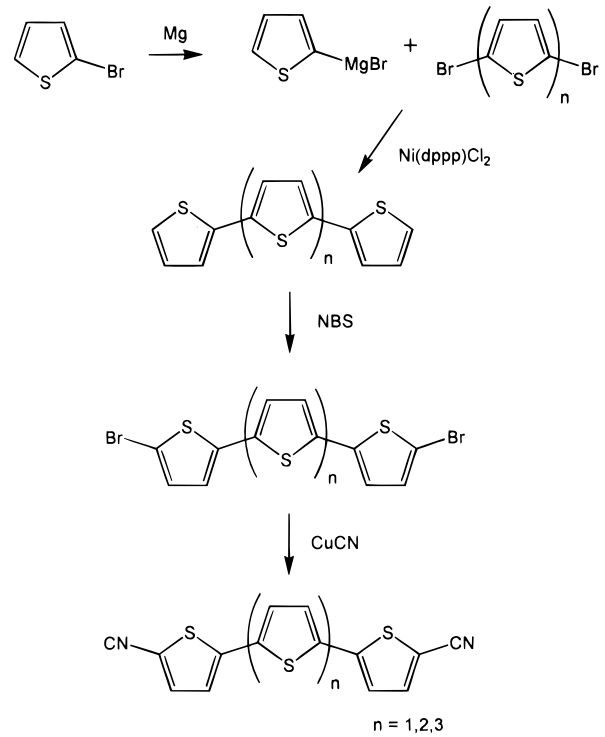

The preparation of $(CN)_2T_n$ ($n = 3-5$) is outlined in Scheme 1. As a first step the Grignard reagent prepared from 2-bromothiophene was added to a solution of the dibromooligothiophene Br_2T_n ($n = 1-3$) containing the Kumada coupling reagent diphenylphosphinopropanenickel(II) chloride.[24] The resulting oligothiophene T_n ($n = 3-5$) was then reacted with 2 equiv of *N*-bromosuccinimide (NBS) in dimethylformamide (DMF) to form the corresponding α,ω-dibromooligothiophene Br_2T_n ($n = 3-5$).[25] The α,ω-dibromo compounds were then converted to α,ω-dinitriles by reaction with copper(I) cyanide in refluxing quinoline.[21,22,26] Isolation and purification of the products required several steps. The reaction mixture was first quenched with aqueous HCl, to protonate and remove the quinoline, and the crude dinitrile isolated from the aqueous phase by filtration. This crude material was then extracted into boiling chlorobenzene and the solution hot filtered. The microcrystalline solid obtained upon cooling was purified by vacuum sublimation in a gradient tube furnace.

Dicyanosexithiophene $(CN)_2T_6$ could not be prepared by this method. Although the synthesis of H_2T_6 itself

(11) Katz, H. E.; Dodabalapur, A.; Torsi, L.; Elder, D. *Chem. Mater.* **1995**, *7*, 2238.
(12) (a) Porzio, W.; Destri, S.; Mascherpa, M.; Bruckner, S. *Acta Polymer.* **1993**, *44*, 266. (b) Porzio, W.; Destri, S.; Mascherpa, M.; Rossini, S.; Bruckner, S. *Synth. Met.* **1993**, *55−57*, 408.
(13) Visser, G. J.; Heeres, G. J.; Wolters, J.; Vos, A. *Acta Crystallogr.* **1968**, *24B*, 467.
(14) van Bolhuis, F.; Wynberg, H.; Havinga, E. E.; Meijer, E. W.; Staring, E. G. J. *Synth. Met.* **1989**, *30*, 381.
(15) Seigrist, T.; Fleming, R. M.; Haddon, R. C.; Laudise, R. A.; Lovinger, A. J.; Katz, H. E.; Bridenbaugh, P.; Davis, D. D. *J. Mater. Res.* **1995**, *10*, 2170.
(16) Horowitz, G.; Bachet, B.; Yassar, A.; Lang, P.; Demanze, F.; Fave, J.-L.; Garnier, F. *Chem. Mater.* **1995**, *7*, 1337.
(17) Fichou, D.; Bachet, B.; Demanze, F.; Billy, I.; Horowitz, G.; Garnier, F. *Adv. Mater.* **1996**, *8*, 500.
(18) Hotta, S.; Waragai, K. *J. Mater. Chem.* **1991**, *1*, 835.
(19) Yassar, A.; Garnier, F.; Deloffre, F.; Horowitz, G.; Ricard, L. *Adv. Mater.* **1994**, *6*, 660.
(20) Reddy, D. S.; Ovchinnikov, Y. E.; Shishkin, O. V.; Struchkov, Y. T.; Desiraju, G. R. *J. Am. Chem. Soc.* **1996**, *118*, 4085.
(21) Paulmier, C.; Morel, J.; Pastour, P. *Bull. Chem. Soc. Fr.* **1969**, 2511.
(22) Pedulli, G. F.; Tiecco, M.; Guerra, M.; Martelli, G.; Zanirato, P. *J. Chem. Soc., Perkin Trans. 2* **1978**, 212.
(23) Demanze, F.; Godillot, P.; Garnier, F.; Hapiot, P. *J. Electroanal. Chem.* **1996**, *414*, 61.
(24) (a) Tamao, K.; Sumitani, K.; Kiso, Y.; Zembayashi, M.; Fujioka, A.; Kodama, S.; Nakajima, I.; Minato, A.; Kumada, M. *Bull. Chem. Soc. Jpn.* **1976**, *49*, 1958. (b) Tamao, K.; Kodama, S.; Makajima, I.; Kumada, M.; Minato, A; Suzuki, K. *Tetrahedron* **1982**, *38*, 3347.
(25) Bäuerle, P.; Würthner, F.; Götz, G.; Effenberger, F. *Synthesis* **1993**, 1099.
(26) Cordes, A. W.; Haddon, R. C.; MacKinnon, C. D.; Oakley, R. T.; Patenaude, G. W.; Reed, R. W.; Rietveld, T.; Vajda, K. E. *Inorg. Chem.* **1996**, *35*, 7626.

Scheme 2

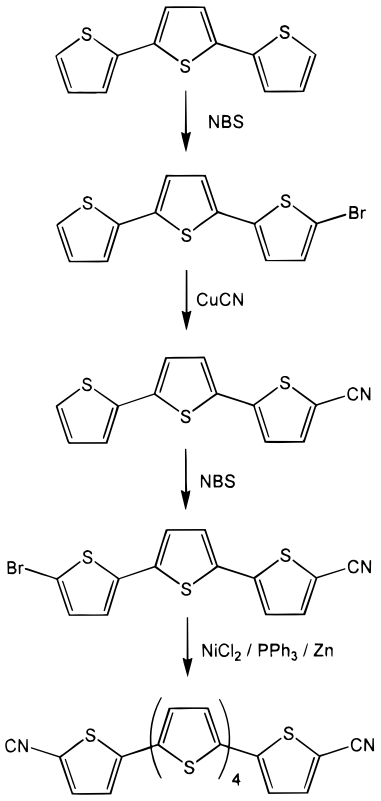

is well-known,[27] it is highly insoluble and bromination with NBS must be carried out at a temperature (120 °C, DMF) that leads to H−Br exchange at the 3- and 4-positions on the terminal thiophene residues. The resulting mixture of isomers of multiply brominated sexithiophenes is impossible to separate and purify. The synthetic route outlined in Scheme 2 was therefore developed. As a first step terthiophene was monobrominated by the slow addition of NBS at −20 °C.[25] This reaction takes advantage of the fact that the monobrominated product is much less soluble in DMF at low temperature than is terthiophene itself. The product, monobromoterthiophene HT_3Br, was then converted to cyanoterthiophene $(CN)T_3H$ and the latter subsequently oxidized with NBS to produce bromocyanoterthiophene $(CN)T_3Br$. This compound was then added to the homocoupling catalyst nickel(0) tris(triphenylphosphine), generated in situ from nickel dichloride, triphenylphosphine, and zinc.[28] Finally the crude $(CN)_2T_6$ was purified by extraction into and crystallization from hot benzonitrile. The compound was further purified by vacuum sublimation in a gradient tube furnace.

Crystal Structures. While there have been relatively few structural determinations on oligothiophenes,[13−19] the factors affecting the packing of polycyclic aromatic structures in general are well understood. The propensity of molecules such as naphthalene,[29] anthracene,[30] and biphenyl[31] to adopt herringbone patterns have been explained in terms of structure-making edge-to-face (tilted-T) aromatic interactions.[32] These are attractive London dispersion effects.[33] The observation of herringbone packing patterns in H-substituted oligothiophene crystals and films[34] thus holds few interpretational surprises. The incorporation of dicyano end-groups, however, changes the complexion of the molecules. The ability of nitrile residues to act as supramolecular synthons, i.e., to exert structure-making interactions, with halogens, chalcogens, and (C)−H groups is well documented,[20,35] and in the structures reported here intermolecular CN- - -H interactions link oligothiophene molecules into extended ribbons. For the shorter chains ($n = 3-5$) these links, which are the pairwise type illustrated in **1**, enforce approximate coplanarity of consecutive oligomeric units along these ribbonlike arrays, so that the molecules adopt slipped π-stack motifs rather than herringbone structures. These issues are elaborated below.

To date there has been no structural investigation on any α,ω-dicyanooligothiophene $(CN)_2T_n$. In this work we have focused on the longer chain oligomers ($n = 3-6$), so as to be able to make direct comparison with the corresponding proto-substituted compounds H_2T_n. Crystals of $(CN)_2T_n$ ($n = 3-6$) suitable for X-ray work were grown by fractional sublimation in vacuo. All samples were prepurified by crystallization, from chlorobenzene or benzonitrile, and doubly sublimed in vacuo in a gradient tube furnace. Specific temperature conditions are provided in the Experimental Section. To suppress twinning, very slow sublimation periods (1−3 weeks for 200−400 mg) were required for all four compounds studied. In all cases the crystals selected for X-ray analysis were typical of the bulk; we observed no indication of polymorphism. Atomic coordinates for the four structures are compiled in Tables 1−4. Selected intramolecular distances are summarized in Table 5. Collectively and individually the CN, C−C(N), and backbone (C3−C4) distances suggest little quinoidal[36] involvement in the ground-state structure. All four crystal structures consist of approximately planar molecules in which the thiophene rings are oriented in an all-trans conformation. Details of individual structures follow.

$(CN)_2T_3$. The crystals belong to the monoclinic space group *C*2/*c*, with 2.5 molecules in the asymmetric unit (one molecule is located on a crystallographic 2-fold rotation axis). Figure 1a shows a side view of these ribbonlike arrays of $(CN)_2T_3$ units and illustrates how molecules in different layers form slipped π-stacks. The presence of 2.5 crystallographically independent molecules per asymmetric unit allows this stacking to consist of five-molecule layers (a 5-stack), within which there is a lateral shift (sideways slippage) of one-half

(27) (a) Kagan, J.; Arora, S. K. *Heterocycles* **1983**, *20*, 1937. (b) Nakayama, J.; Konishi, T.; Murabayashi, S.; Hoshino, M. *Heterocycles* **1987**, *26*, 1793. (c) Fichou, D.; Horowitz, G. G.; Garnier, F. Eur. Pat. Appl. EP 402,269, 1990; *Chem. Abstr.* **1991**, *114*, 186387g.
(28) Colon, I.; Kelsey, D. R. *J. Org. Chem.* **1986**, *51*, 2627.
(29) Dunitz, J. D.; Brock, C. P. *Acta Crystallogr.* **1982**, *38B*, 2218.
(30) Brock, C. P.; Dunitz, J. D. *Acta Crystallogr.* **1990**, *46B*, 795.
(31) Hargreaves, A.; Rizvi, S. *Acta Crystallogr.* **1962**, *15*, 365.
(32) See, for example: (a) Burley, S. K.; Petsko, G. A. *Science* **1985**, *229*, 23. (b) Gavezotti, A.; Desiraju, G. R. *Acta Crystallogr.* **1988**, *44B*, 427. (c) Bernstein, J.; Sarma, J. A. R. P.; Gavezotti, *Chem. Phys. Lett.* **1990**, *174*, 361. (d) Hobza, P.; Selze, H. L.; Schlag, E. W. *J. Am. Chem. Soc.* **1994**, *116*, 3500. (e) Jorgensen, W. L.; Severance, D. L. *J. Am. Chem. Soc.* **1989**, *112*, 4768.
(33) Paliwal, S.; Geib, S.; Wilcox, C. S. *J. Am. Chem. Soc.* **1994**, *116*, 4497.
(34) Taliani, C.; Blinov, L. M. *Adv. Mater.* **1996**, *8*, 353.
(35) (a) Cordes, A. W.; Haddon, R. C.; Hicks, R. G.; Oakley, R. T.; Palstra, T. T. M. *Inorg. Chem.* **1992**, *31*, 1802. (b) Cordes, A. W.; Haddon, R. C.; Hicks, R. G.; Kennepohl, D. K.; Oakley, R. T.; Palstra, T. T. M.; Schneemeyer, L. F.; Scott, S. R.; Waszczak, J. V. *Chem. Mater.* **1993**, *5*, 820.
(36) Alemán, C.; Julià, L. *J. Phys. Chem.* **1996**, *100*, 14661.

Table 1. Non-hydrogen Atomic Parameters *x, y, z,* and B_{eq} for $(CN)_2T_3$[a]

	x	*y*	*z*	B_{eq}
S1	0.79728(18)	0.1482(2)	0.04810(9)	4.43(17)
S2	0.80162(17)	0.0074(2)	0.17973(8)	3.93(17)
S3	0.79184(18)	0.2097(2)	0.29698(10)	4.45(18)
S4	0.58952(19)	0.1114(2)	−0.02592(9)	4.88(18)
S5	0.60345(18)	−0.0147(2)	0.10868(9)	4.08(16)
S6	0.59412(19)	0.2094(2)	0.22029(10)	4.45(18)
S7	0.01047(18)	0.1886(2)	0.12552(10)	4.25(16)
S8	0	0.0180(3)	1/4	3.6(2)
C1	0.8067(7)	0.0676(9)	−0.0333(4)	5.0(7)
C2	0.8067(6)	0.0418(9)	0.0117(3)	3.5(6)
C3	0.8100(7)	−0.0617(9)	0.0318(4)	4.9(7)
C4	0.8060(7)	−0.0543(9)	0.0764(4)	4.8(7)
C5	0.8007(6)	0.0544(9)	0.0906(3)	3.5(6)
C6	0.7979(6)	0.0971(9)	0.1349(3)	3.3(6)
C7	0.7961(6)	0.2047(9)	0.1486(4)	4.6(6)
C8	0.7944(7)	0.2194(8)	0.1936(4)	4.6(7)
C9	0.7983(6)	0.1182(8)	0.2161(3)	3.1(6)
C10	0.7990(6)	0.0990(8)	0.2628(3)	3.2(6)
C11	0.8040(6)	−0.0019(8)	0.2852(3)	3.9(6)
C12	0.8011(6)	0.0122(9)	0.3309(3)	4.3(7)
C13	0.7955(6)	0.1223(8)	0.3427(3)	3.4(6)
C14	0.7929(7)	0.1661(10)	0.3858(3)	4.3(6)
C15	0.6003(8)	0.0279(10)	−0.1058(4)	5.5(7)
C16	0.6017(7)	0.0045(9)	−0.0608(4)	4.3(6)
C17	0.6146(8)	−0.0911(10)	−0.0396(4)	6.0(8)
C18	0.6133(6)	−0.0850(9)	0.0051(4)	4.6(7)
C19	0.6004(6)	0.0191(9)	0.0193(3)	3.6(6)
C20	0.5949(6)	0.0662(9)	0.0620(3)	3.5(6)
C21	0.5856(8)	0.1759(10)	0.0718(4)	6.5(8)
C22	0.5843(8)	0.1943(9)	0.1165(4)	6.0(8)
C23	0.5937(6)	0.0989(9)	0.1408(3)	3.8(6)
C24	0.5960(6)	0.0887(8)	0.1882(4)	3.5(6)
C25	0.6018(7)	−0.0035(9)	0.2144(3)	4.6(6)
C26	0.6025(6)	0.0214(9)	0.2597(3)	4.1(6)
C27	0.6004(6)	0.1333(10)	0.2679(4)	4.0(6)
C28	0.6027(6)	0.1870(9)	0.3100(4)	4.2(7)
C29	0.0157(7)	0.1191(8)	0.0407(4)	4.2(6)
C30	0.0069(6)	0.0876(9)	0.0843(3)	3.5(6)
C31	−0.0018(6)	−0.0166(10)	0.0997(3)	4.0(6)
C32	−0.0065(7)	−0.0170(9)	0.1442(4)	4.4(6)
C33	−0.0008(5)	0.0859(9)	0.1638(3)	3.4(6)
C34	−0.0011(6)	0.1194(10)	0.2099(3)	3.4(6)
C35	−0.0016(7)	0.2234(8)	0.2272(3)	4.3(6)
N1	0.8075(7)	0.0911(9)	−0.0690(3)	7.4(7)
N2	0.7908(6)	0.2020(9)	0.4187(4)	7.0(7)
N3	0.5978(7)	0.0600(9)	−0.1412(3)	7.2(8)
N4	0.6036(6)	0.2324(8)	0.3423(3)	5.9(6)
N5	0.0230(6)	0.1459(9)	0.0067(3)	6.6(7)

[a] ESDs refer to the last digit printed. B_{eq} is the mean of the principal axes of the thermal ellipsoid.

Table 2. Non-hydrogen Atomic Parameters *x, y, z,* and B_{eq} for $(CN)_2T_4$[a]

	x	*y*	*z*	B_{eq}
S1	0.24948(8)	0.35983(9)	0.45425(8)	4.20(3)
S2	0.85706(8)	0.30480(8)	0.25525(8)	4.13(3)
N1	−0.1354(3)	0.1452(3)	0.8329(3)	5.39(12)
C1	0.0170(3)	0.1625(3)	0.7610(3)	3.92(10)
C2	0.2064(3)	0.1856(3)	0.6696(3)	3.49(10)
C3	0.3708(4)	0.0800(4)	0.7300(3)	4.26(12)
C4	0.5327(3)	0.1422(4)	0.6022(3)	4.17(12)
C5	0.4904(3)	0.2942(3)	0.4468(3)	3.24(10)
C6	0.6195(3)	0.3967(3)	0.2847(3)	3.15(10)
C7	0.5817(3)	0.5647(3)	0.1438(3)	4.22(11)
C8	0.7432(3)	0.6215(3)	0.0116(3)	4.29(11)
C9	0.9042(3)	0.4954(3)	0.0512(3)	3.23(10)

[a] ESDs refer to the last digit printed. B_{eq} is the mean of the principal axes of the thermal ellipsoid.

of a thiophene ring per layer. Lateral slippage of neigboring 5-stacks corresponds to about one-half of a $(CN)_2T_3$ molecule. Within these slipped stack arrays there are numerous intermolecular S- - -S contacts below 4 Å; these lie in the range 3.824−3.985 Å, with

Table 3. Non-hydrogen Atomic Parameters *x, y, z,* and B_{eq} for $(CN)_2T_5$[a]

	x	*y*	*z*	B_{eq}
S1	0.71660(11)	0.28566(13)	0.72606(4)	5.27(8)
S2	0.56192(10)	0.50209(12)	0.80251(4)	4.12(7)
S3	0.37578(10)	0.37007(13)	0.88779(4)	4.41(7)
S4	0.23248(11)	0.55617(13)	0.97420(4)	4.30(7)
S5	0.04858(11)	0.39429(12)	1.05490(4)	4.64(7)
S6	0.83646(11)	0.17926(12)	0.08282(4)	4.66(7)
S7	0.66511(10)	0.00608(13)	0.16525(3)	4.18(7)
S8	1/2	0.17701(16)	1/4	4.21(10)
C1	0.8336(4)	0.3179(5)	0.66716(15)	4.4(3)
C2	0.7760(3)	0.3686(5)	0.69578(13)	3.8(2)
C3	0.7609(4)	0.4794(5)	0.70197(14)	4.8(3)
C4	0.7006(4)	0.4996(5)	0.73186(14)	4.7(3)
C5	0.6709(3)	0.4034(4)	0.74812(12)	3.4(2)
C6	0.6099(4)	0.3875(4)	0.77954(13)	3.5(2)
C7	0.5815(4)	0.2899(5)	0.79568(14)	5.1(3)
C8	0.5234(4)	0.3045(5)	0.82565(16)	5.4(3)
C9	0.5057(4)	0.4147(5)	0.83360(13)	3.7(3)
C10	0.4499(3)	0.4608(5)	0.86334(13)	3.4(2)
C11	0.4457(4)	0.5663(5)	0.87662(14)	4.6(3)
C12	0.3823(4)	0.5765(5)	0.90731(15)	5.2(3)
C13	0.3405(3)	0.4763(5)	0.91578(12)	3.7(3)
C14	0.2723(4)	0.4521(5)	0.94582(13)	3.7(3)
C15	0.2317(4)	0.3502(5)	0.95377(15)	5.1(3)
C16	0.1688(4)	0.3552(5)	0.98384(15)	5.1(3)
C17	0.1616(4)	0.4610(4)	0.99862(13)	3.4(2)
C18	0.1050(3)	0.4971(5)	1.02896(13)	3.4(2)
C19	0.0859(4)	0.6019(5)	1.04231(14)	4.5(3)
C20	0.0269(4)	0.6017(5)	1.07247(14)	4.6(3)
C21	−0.0001(4)	0.4973(5)	1.08251(13)	3.8(2)
C22	−0.0612(4)	0.4627(5)	1.11172(14)	4.4(3)
C23	0.9453(4)	0.1149(5)	0.02515(14)	4.3(3)
C24	0.8874(4)	0.0798(5)	0.05502(13)	3.8(2)
C25	0.8641(4)	−0.0278(5)	0.06513(14)	4.6(3)
C26	0.8058(4)	−0.0309(5)	0.09559(14)	4.2(3)
C27	0.7830(3)	0.0739(5)	0.10884(12)	3.3(2)
C28	0.7246(4)	0.1073(4)	0.13935(13)	3.5(2)
C29	0.7059(4)	0.2122(5)	0.15219(14)	4.7(3)
C30	0.6439(4)	0.2132(5)	0.18253(14)	5.0(3)
C31	0.6159(4)	0.1074(4)	0.19254(13)	3.6(2)
C32	0.5533(3)	0.0769(4)	0.22303(12)	3.3(2)
C33	0.5316(4)	−0.0299(5)	0.23436(15)	5.2(3)
N1	0.8779(4)	0.2747(4)	0.64620(14)	6.3(3)
N2	−0.1113(4)	0.4315(4)	1.13392(13)	6.2(3)
N3	0.9915(4)	0.1460(4)	0.00198(13)	5.7(3)

[a] ESDs refer to the last digit printed. B_{eq} is the mean of the principal axes of the thermal ellipsoid.

Table 4. Non-hydrogen Atomic Parameters *x, y, z,* and B_{eq} for $(CN)_2T_6$[a]

	x	*y*	*z*	B_{eq}
S1	0.56498(8)	0.6775(2)	0.17182(9)	3.58(6)
S2	0.30463(9)	0.3674(2)	0.25300(9)	3.50(5)
S3	0.12515(8)	0.66376(19)	0.45132(8)	3.09(5)
C1	0.7094(4)	0.5356(9)	0.0732(4)	4.3(2)
C2	0.6175(3)	0.4866(8)	0.1024(3)	3.25(19)
C3	0.5631(3)	0.2973(8)	0.0849(3)	3.6(2)
C4	0.4781(3)	0.3020(7)	0.1271(3)	3.01(19)
C5	0.4686(3)	0.4978(7)	0.1777(3)	2.65(16)
C6	0.3947(3)	0.5578(7)	0.2363(3)	2.61(18)
C7	0.3857(3)	0.7508(8)	0.2866(3)	3.29(19)
C8	0.3080(3)	0.7444(8)	0.3406(3)	3.23(19)
C9	0.2571(3)	0.5477(7)	0.3309(3)	2.67(18)
C10	0.1732(3)	0.4802(7)	0.3750(3)	2.81(17)
C11	0.1222(3)	0.2826(8)	0.3650(3)	3.4(2)
C12	0.0442(3)	0.2759(7)	0.4180(3)	3.11(19)
C13	0.0355(3)	0.4718(7)	0.4693(3)	2.72(18)
N	0.7845(3)	0.5711(10)	0.0524(4)	6.6(3)

[a] ESDs refer to the last digit printed. B_{eq} is the mean of the principal axes of the thermal ellipsoid.

the exception of S1- - -S4′, which is 3.671 Å. Figure 2a shows a view of the packing parallel to the *z* direction and the approximately out-of-register arrangement of ribbons within adjacent sheets. Along the ribbonlike

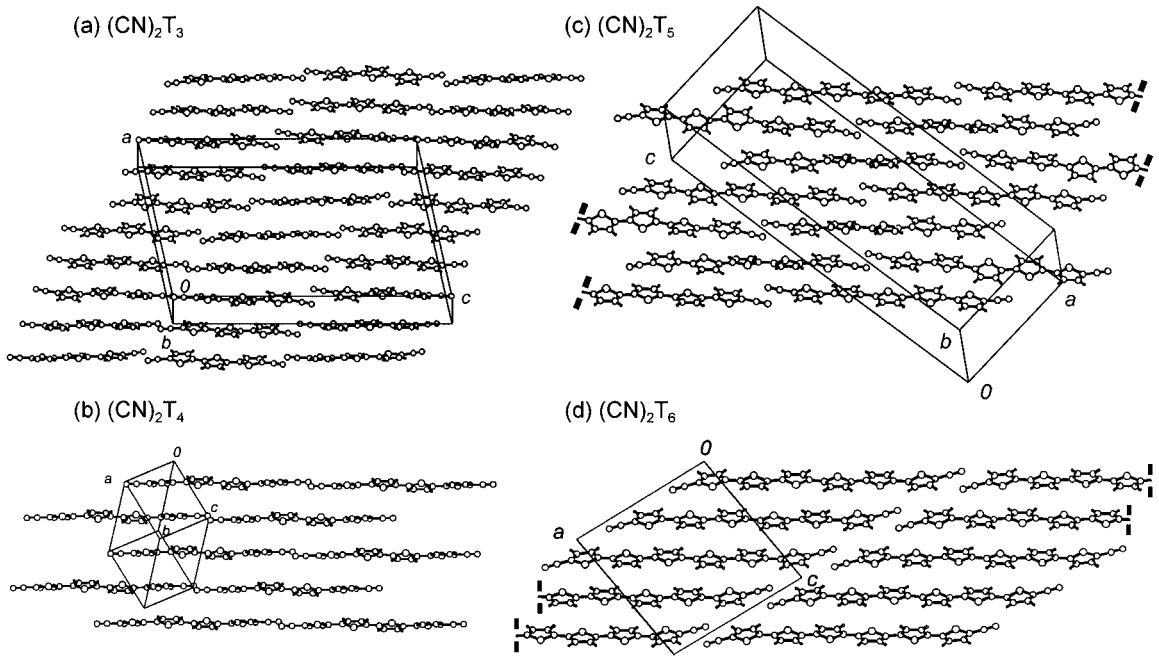

Figure 1. Side view of packing in $(CN)_2T_n$ ($n = 3-6$) showing ribbonlike arrays.

Table 5. Summary of Intramolecular Distances (Å) in $(CN)_2T_n$ ($n = 3-6$)

compound	C−N		C−C(N)		C−C(backbone)	
$(CN)_2T_3$	C1−N1	1.131(17)	C1−C2	1.415(17)	C3−C4	1.389(16)
	C14−N2	1.102(15)	C13−C14	1.431(15)	C17−C18	1.396(15)
	C15−N3	1.142(16)	C15−C16	1.403(16)	C11−C12	1.424(13)
	C28−N4	1.124(16)	C27−C28	1.433(17)	C17−C18	1.376(16)
	C29−N5	1.125(15)	C26−C30	1.430(15)	C21−C22	1.395(16)
					C25−C26	1.417(14)
					C31−C32	1.384(14)
					C35−C35′	1.385(19)
	av	1.125	av	1.422	av	1.396
$(CN)_2T_4$	C1−N	1.139(3)	C1−C2	1.420(3)	C3−C4	1.404(3)
					C7−C8	1.408(3)
					av	1.406
$(CN)_2T_5$	C1−N1	1.109(7)	C1−C2	1.450(7)	C3−C4	1.404(7)
	C22−N2	1.133(7)	C21−C22	1.429(7)	C7−C8	1.379(7)
	C23−N3	1.128(7)	C23−C24	1.424(7)	C11−C12	1.438(7)
					C15−C16	1.411(7)
					C19−C20	1.381(7)
					C25−C26	1.385(7)
					C29−C30	1.411(7)
					C33−C33′	1.448(9)
	av	1.123	av	1.434	av	1.407
$(CN)_2T_6$	C1−N	1.145(7)	C1−C2	1.427(7)	C3−C4	1.399(6)
					C7−C8	1.410(6)
					C11−C12	1.403(6)
					av	1.404

arrays neighboring molecules are bridged by intermolecular CN- - -H interactions (all as in **1**). In addition to S- - -S′ contacts there are numerous S- - -C′ contacts, the shortest (S3- - -C27′) being 3.557 Å.

$(CN)_2T_4$. The crystals are triclinic, space group $P\bar{1}$, with 0.5 molecule/asymmetric unit (the molecule is located on a crystallographic inversion center). As a result the structure is simpler than that of the corresponding terthiophene. Nonetheless, as illustrated in Figure 1b, the structure again consists of a ribbonlike network of molecules which gives rise to a slipped π-stack assembly. The lateral slippage in this system is more marked than in $(CN)_2T_3$, amounting to 0.5 molecule/layer. The intermolecular CN- - -H interactions (as in **1**) that link consecutive molecules along the chain are 2.686 Å. Figure 2b shows the stacking of the ribbons in $(CN)_2T_4$; in this case the ribbons in adjacent stacks are in-register. There are two S- - -S′ contacts, S1- - -S1′ (3.894 Å) and S1- - -S2′ (3.812 Å) below 4 Å, as well as a series of four short S- - -C′ within the range 3.630−3.738 Å.

$(CN)_2T_5$. Like $(CN)_2T_3$, crystals of $(CN)_2T_5$ belong to the monoclinic space group $C2/c$, but in this case there are 1.5 molecules/asymmetric unit (one molecule is located on a crystallographic 2-fold rotation axis). Figure 1c illustrates the ribbonlike arrays and π-stacking of the molecular ribbons, while Figure 2c shows the approximately out-of-register packing of ribbons in adjacent stacks. Lateral slippage in this system is similar to that found in $(CN)_2T_4$, i.e., about 0.5 molecule/layer. Along the ribbonlike arrays neighboring molecules are bridged by intermolecular CN- - -H interactions (all as in **1**). In this structure the shortest S- - -S′

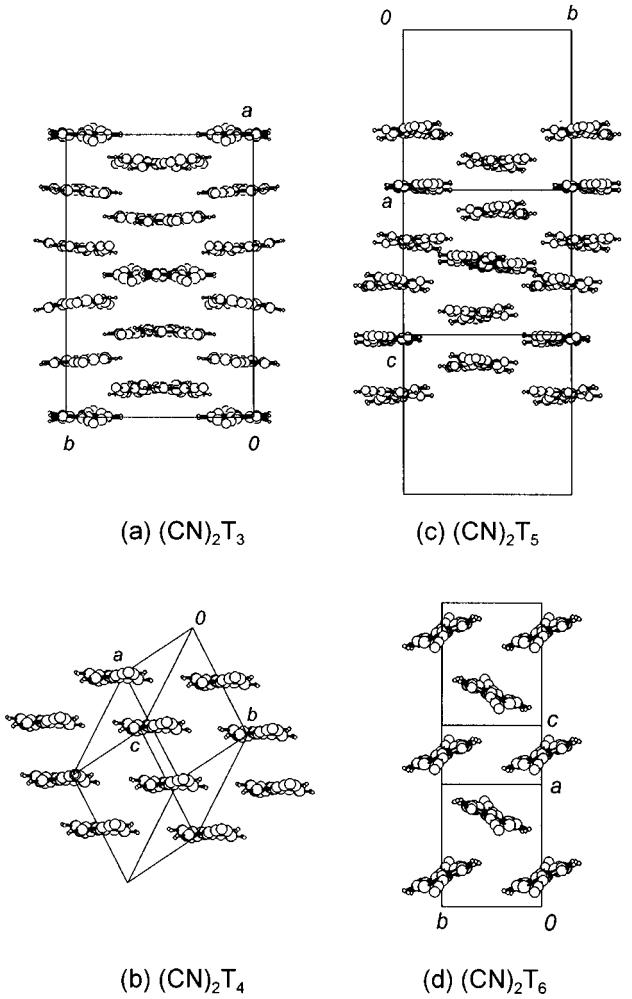

Figure 2. End view of ribbons in $(CN)_2T_n$, showing out-of-register layers in $(CN)_2T_n$ (n = 3 and 5), in-register layers in $(CN)_2T_4$, and herringbone packing in $(CN)_2T_6$.

contact (S4- - -S6′) is 3.864 Å and the shortest four S- - -C′ contacts lie in the range 3.529−3.693 Å.

$(CN)_2T_6$. Crystals of $(CN)_2T_6$ belong to the monoclinic space group $P2_1/a$, with 0.5 molecule/asymmetric unit (the molecule is located on a crystallographic inversion center). In contrast to the shorter chain compounds, $(CN)_2T_6$ does *not* adopt the slipped π-stack structure. While ribbons formed by molecules (Figure 1d) linked by CN- - -H contacts (2.592 Å) are still observed, the coupling pattern differs from that illustrated in **1**. Instead of there being pairs of CN- - -H between molecules in the same ribbon, the CN- - -H contacts are offset to form the interlocking pattern shown in Figure 3. This arrangement allows consecutive molecules along a given ribbon strand to rotate (plus and minus) about the ribbon axis, so that the herringbone packing pattern (of H_2T_6) can develop. The end-view of the ribbons (Figure 2d) also illustrates this rotation of the molecules about the molecular (and ribbon) axis. As a result of the absence of stacking observed in the shorter chain compounds, there are no S- - -S′ contacts below 4 Å, but there are a series of four S- - -C′ contacts ranging from 3.584 to 3.744 Å.

UV−Visible Spectroscopy. Recent electrochemical studies on $(CN)_2T_n$ (n = 2, 3) have shown that the first reduction potentials undergo cathodic shifts, of 360 and 220 mV, respectively, relative to the parent oligothiophenes H_2T_n.[37] Oxidation potentials are also strongly shifted to less positive values, in accord with expected electron-acceptor properties of the nitrile group. These shifts in redox potentials can be expected to continue, but to diminishing extents, with increasing chain length, but the low solubility of all the compounds with $n > 3$ have thwarted our attempts to obtain electrochemical data for the longer chains.[23] However, given the high extinction coefficients for the low-energy $\pi-\pi^*$ excitation of $(CN)_2T_n$ (n = 2−6), we have been able to dissolve sufficient quantities of the compounds in DMSO to allow measurement of their UV−visible spectra. These spectra, coupled with the results of MNDO calculations on both $(H)_2T_n$ and $(CN)_2T_n$ (n = 2−6) provide a qualitative insight into the way in which the nitrile end-groups affect the ground state donor/acceptor properties[38] of the oligothiophene chain.

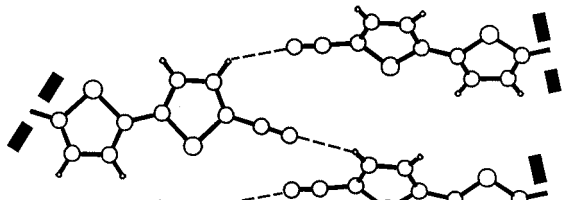

Figure 3. Offsetting of intermolecular CN- - -H interactions in $(CN)_2T_6$. The mutual rotation of adjacent molecules in $(CN)_2T_6$ is also illustrated.

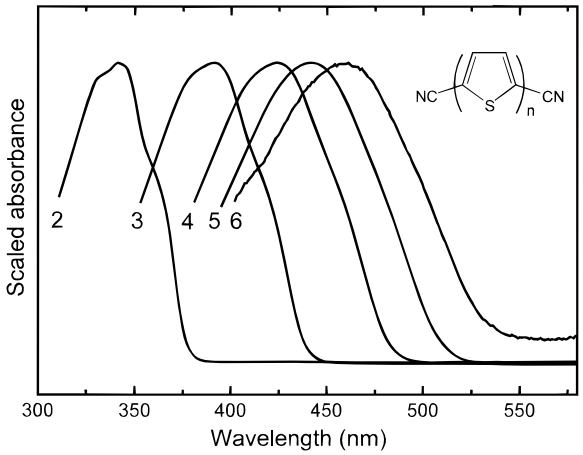

Figure 4. UV−visible spectra of $(CN)_2T_n$ (n = 3−6), in DMSO. Absorbance maxima are set to a common value for ease of comparison.

The UV−visible spectra are illustrated in Figure 4, and λ_{max} values are reported in Table 6, along with the corresponding values for other α,ω-disubstituted oligothiophenes $(R)_2T_n$ (n = 2−6) (R = H,[27b,38−40] CH_3,[18] CH_2NH_2,[41] OMe,[38] NO_2,[38] CHO[42]). As expected, the attachment of the strongly electron-withdrawing cyano end-

(37) Hapiot, P.; Demanze, F.; Yassar, A.; Garnier, F. *J. Phys. Chem.* **1996**, *100*, 8397.
(38) Garcia, P.; Pernaut, J. M.; Hapiot, P.; Wintgens, V.; Valat, P.; Garnier, F.; Delabouglise, D. *J. Phys. Chem.* **1993**, *97*, 513.
(39) Grebner, D.; Helbig, M.; Rentsch, S. *J. Phys. Chem.* **1995**, *99*, 16991.
(40) (a) Fichou, D.; Horowitz, G.; Nishikitani, Y.; Garnier, F. *Synth. Met.* **1989**, *28*, C723. (b) Houben, J. L.; Cimiraglia, R.; Carpita, A.; Ciofalo, M. *J. Mol. Liq.* **1994**, *61*, 189. (c) Sease, J. W.; Zechmeister, L. *J. Am. Chem. Soc.* **1947**, *69*, 270.

Table 6. Band Maxima for Lowest Energy $\pi-\pi^*$ Excitation (λ_{max}, nm) for α,ω-Disubstituted Oligothiophenes R_2T_n

	n				
R	2	3	4	5	6
H[a]	302	355	390	416	432
CH_3[b]	316	364	397	422	
CH_2NH_2[c]	320	367	400	423	
OMe[d]	332		405		442
NO_2[d]					465
CHO[e]		414	440	456	461
CN[f]	341	391	423	442	461

[a] In $CHCl_3$.[39] See also refs 27b, 38, 40, and 46. [b] In CH_2Cl_2.[18] [c] In CH_2Cl_2.[41] [d] In CH_2Cl_2.[38] [e] In CH_2Cl_2.[42] [f] In DMSO, this work.

Table 7. Calculated (MNDO) Shifts (Δ, eV) in Frontier Orbital Energies (ϵ, eV) between α,ω-H_2T_n and α,ω-$(CN)_2T_n$ ($n = 2-6$)[a]

n		α,ω-H_2T_n	α,ω-$(CN)_2T_n$	Δ[b]
2	ϵ(LUMO)	−0.764 (a_u)	−1.774 (a_u)	1.010
	ϵ(HOMO)	−8.712 (b_g)	−9.402 (b_g)	0.690
3	ϵ(LUMO)	−1.106 (b_1)	−1.826 (b_1)	0.720
	ϵ(HOMO)	−8.420 (a_2)	−8.968 (a_2)	0.548
4	ϵ(LUMO)	−1.287 (a_u)	−1.831 (a_u)	0.544
	ϵ(HOMO)	−8.280 (b_g)	−8.722 (b_g)	0.442
5	ϵ(LUMO)	−1.393 (b_1)	−1.818 (b_1)	0.425
	ϵ(HOMO)	−8.207 (a_2)	−8.564 (a_2)	0.357
6	ϵ(LUMO)	−1.461 (a_u)	−1.803 (a_u)	0.342
	ϵ(HOMO)	−8.165 (b_g)	−8.459 (b_g)	0.294

[a] Geometries are fully optimized within C_{2h} (*n* even) and C_{2v} (*n* odd) symmetry. [b] $\Delta = \epsilon(\alpha,\omega\text{-}H_2T_n) - \epsilon(\alpha,\omega\text{-}(CN)_2T_n)$.

groups induces bathochromic shifts of 20−40 nm relative to the proto and alkyl derivatives. To the extent that the data available for the dimethoxy, dinitro, and diformyl compounds allows comparison, the shifts induced by nitrile groups (i.e., R = CN in R_2T_n) are substantially larger than for R = OMe and comparable to R = NO_2 and CHO. Nitrile groups on β-hexyl-substituted oligothiophenes also produce red-shifts.[43] However, in these systems the effect is smaller, as the hexyl groups induce a twisting of the oligothiophene, thereby disrupting conjugation between consecutive rings.

There have been numerous theoretical investigations on the excited states of oligothiophenes.[44,45] In this work we have carried out MNDO calculations on both H_2T_n and $(CN)_2T_n$ ($n = 2-6$) and monitored the changes in the HOMO/LUMO energies as a guide both to spectral shifts and donor/acceptor behavior. The MNDO method has been used previously to study the geometries[14,46] and occupied orbital manifolds[46] of H_2T_n. It gives reliable predictions of structural features and ionization potentials. Table 7 provides the MNDO eigenvalues and symmetries of the highest occupied and lowest unoccupied molecular orbitals (HOMO and LUMO) for the two series. Although we have not performed any excited-state calculations, the symmetries of the HOMO/LUMO pairs are such that HOMO−LUMO excitations give rise, in all cases, to excited-state symmetries that match those obtained recently from CNDO/S calculations on $(H)_2T_n$,[45] i.e., the lowest excited singlet state is of B_u (for $n = 2, 4, 6$) and B_2 (for $n = 3, 5$) symmetry. Moreover, while we cannot relate the size of the HOMO−LUMO gap from a Hartree−Fock calculation directly to the $\pi-\pi^*$ excitation energy, variations in the orbital eigenvalues can be used to predict trends. Both the HOMO and the LUMO of oligothiophenes have nonzero coefficients at the terminal (2-position) carbons, although that of the HOMO is marginally larger. As a result there is substantial mixing of the nitrile-acceptor level with both orbitals. Mixing with the LUMO is, however, stronger because of the closer energy match between the LUMO and the π^*-acceptor level of the nitrile. Thus, while both the HOMO and LUMO of $(H)_2T_n$ are both lowered in energy in $(CN)_2T_n$, stabilization of the latter predominates, and it is this extra stabilization of the LUMO that leads to the observed diminution in the excitation energy.

The computational and spectral results thus confirm the strong perturbation exerted by the nitrile end-groups on both ground- (redox) and excited-state properties. As already noted for $n = 2$ and 3,[37] the nitrile group induces large cathodic shifts in both reduction and oxidation potentials. The magnitudes of these end-group effects are predicted to diminish with increasing chain length,[23] so that fine-tuning of both molecular and solid-state properties, by modification of both the molecular chain length and the end group, should be possible. In particular the increased electron affinity of dicyanooligothiophenes may lead to useful device applications.[47]

Band Structure Calculations. As the crystal structures of $(CN)_2T_n$ ($n = 3-6$) illustrate, the nitrile moiety plays an important structural role; it orients the oligothiophene chains into ribbonlike arrays in which consecutive molecules are linked by weak CN- - -H interactions. In the case of $n = 3$, 4, and 5 the resultant ribbons form slipped stacks in which consecutive layers are approximately coplanar. For $n = 6$ the ribbons are twisted, and a cross-sectional view parallel to the ribbon direction reveals a herringbone pattern. These differences in molecular packing will clearly play an important role in determining the solid-state properties of the materials. To probe the electronic consequences of these different packing modes we have carried out extended Hückel calculations on the structures of $(CN)_2T_4$ and $(CN)_2T_6$. These two structures, both of which are centrosymmetric, with only 0.5 molecule/asymmetric unit, afford relatively simple electronic band manifolds and are representative of the two stacking modes.

Dispersion along the three principal axes of the reciprocal lattice for the highest lying occupied and lowest lying unoccupied bands are shown, for $(CN)_2T_4$ and $(CN)_2T_6$, in Figures 5 and 6. The results suggest that both materials are indirect semiconductors, with bandgaps of 2.14 ($n = 4$) and 1.88 eV ($n = 6$). The latter

(41) Muguruma, H.; Saito, T.; Sasaki, S.; Hotta, S.; Karube, I. *J. Heterocycl. Chem.* **1996**, *33*, 173.
(42) Wei, Y.; Yang, Y.; Yeh, J.-M. *Chem. Mater.* **1996**, *8*, 2659.
(43) Higuchi, H.; Nakayama, T.; Koyama, H.; Ojima, J.; Wada, T.; Sasabe, H. *Bull. Chem. Soc. Jpn.* **1995**, *68*, 2363.
(44) (a) Belgionne, D.; Shuai, Z.; Bredas, J. L. *J. Chem. Phys.* **1993**, *98*, 8819. (b) Negri, F.; Zgierski, M. Z. *J. Chem. Phys.* **1994**, *100*, 2571. (c) Soos, Z. G.; Galvao, D. S. *J. Phys. Chem.* **1994**, *98*, 1029. (d) Rubio, M.; Merchan, M.; Orti, E.; Roos, B. O. *J. Chem. Phys.* **1995**, *102*, 3580.
(45) Colditz, R.; Grebner, D.; Helbig, M.; Rentsch, S. *J. Inf. Recording* **1996**, *22*, 457.
(46) Fujimoto, H.; Nagashima, U.; Inokuchi, H.; Seki, K.; Cao, Y.; Nakahara, H.; Nakayama, H.; Hoshino, M.; Fukuda, K. *J. Phys. Chem.* **1990**, *92*, 4077.
(47) (a) Greenham, N. C.; Moratti, S. C.; Bradley, D. D. C.; Friend, R. H.; Holmes, A. B. *Nature* **1993**, *365*, 628. (b) Brédas, J. L.; Heeger, A. J.; Wudl, F. *J. Chem. Phys.* **1986**, *85*, 4673.

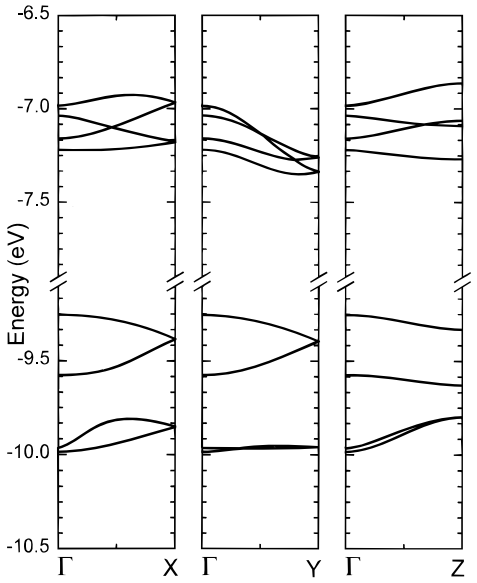

Figure 5. Band dispersion in $(CN)_2T_6$ along the three principal directions of reciprocal space.

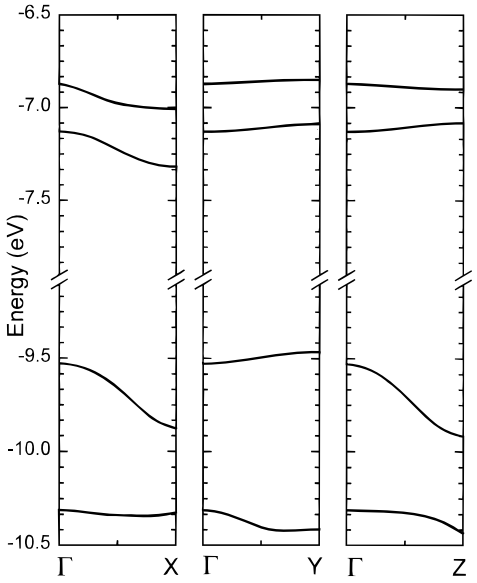

Figure 6. Band dispersion in $(CN)_2T_4$ along the three principal directions of reciprocal space.

value is slightly smaller than that found (1.95 eV) for α-6T/HT.[15] This reduction probably reflects, however, the smaller excitation energy of the molecule (see above) rather than any solid-state feature. The band electronic structure of $(CN)_2T_6$ and α-6T/HT share many common features, as might be expected from the similar packing arrangements. Valence band dispersion for $(CN)_2T_6$ approaches 0.4 eV along *a** and *b**, directions which correspond loosely, in real-space terms, to interactions perpendicular to the molecular chains. This evidence would suggest that $(CN)_2T_6$, like α-6T/HT, has at least a well-developed 2-dimensional electronic structure.

Band dispersion in $(CN)_2T_4$ is harder to interpret. Given that none of the unit cell angles is near 90°, correlation of dispersion along *a**, *b**, or *c** to real-space interactions is less intuitive. Nonetheless, dispersion along *a** and *c** again approaches 0.4 eV, so that a relatively 2-dimensional structure again prevails.

Summary

We have prepared and structurally characterized the α,ω-dicyanooligothiophenes $(CN)_2T_n$ ($n = 3-6$). This series represents the first homologous set of oligothiophenes for which complete single-crystal structural characterization has been achieved. The crystal structures reveal the importance of the nitrile groups in generating molecular ribbons in which the consecutive molecular units are linked by CN- - -H interactions. These CN- - -H interactions appear also to exert an orientational influence on ribbon packing. Thus, at least for the shorter chains ($n = 3$, 4, and 5) the ribbonlike arrays adopt slipped π-stack structures rather than the herringbone packing found in H_2T_3, Me_2T_4, H_2T_6, and H_2T_8. Only for $(CN)_2T_6$ does the packing of the ribbons revert to the herringbone pattern characteristic of the proto (or alkyl) compounds.

The electronic spectra of $(CN)_2T_n$ ($n = 3-6$) show the expected bathochromic shifts in the $\pi-\pi^*$ chromophore, and these data, coupled with computational results on the donor/acceptor levels in the $(CN)_2T_n$ ($n = 3-6$), point to both increased acceptor and decreased donor capabilities of the dicyano compounds relative to the parent proto derivatives. The band structures of $(CN)_2T_n$ ($n =$ 4, 6) suggest substantial intermolecular orbital interactions in both the stacked and herringbone configurations. Future work will establish what effect these end-group modificatons have on solid-state and thin-film transport properties.

Experimental Section

General Procedures and Starting Materials. Copper(I) cyanide, 2-bromothiophene, 2,5-dibromothiophene, [1,3-bis(diphenylphosphino)propane]nickel(II) chloride (Ni(dppp)Cl_2, Aldrich), triphenylphosphine (Kodak), ammonium chloride, hydrochloric acid, magnesium, magnesium sulfate, nickel(II) chloride, and zinc powder (Fisher) were purchased commercially and used as obtained. *N*-Bromosuccinimide (NBS, Fisher) was recrystallized from water, and iodine (Fisher) was sublimed prior to use. The solvents dimethylformamide (DMF), acetonitrile, chlorobenzene, ethanol (95%), quinoline (Fisher), dimethyl sulfoxide (DMSO), and benzonitrile (Aldrich) were used as received. Diethyl ether (Fisher) was freshly dried and distilled over lithium aluminum hydride (Aldrich), and toluene (Fisher) was distilled over sodium (BDH) prior to use. The known compounds 2,2′-bithiophene-5,5′-dicarbonitrile ($(CN)_2T_2$),[22] 2,2′:5′,2″-terthiophene (H_2T_3),[48] 5,5′-dibromo-2,2′-bithiophene (Br_2T_2), 5-bromo-2,2′:5′,2″-terthiophene (HT_3Br), 5,5″-dibromo-2,2′:5′,2″-terthiophene (Br_2T_3), and 5,5‴-dibromo-2,2′:5′,2″:5″,2‴-quaterthiophene (Br_2T_4)[25] were synthesized as prepared previously. Crystals were grown by sublimation in an ATS series 3210 three-zone tube furnace linked to a series 1400 temperature control system. Melting points are uncorrected. ^1H and ^{13}C NMR spectra were recorded on a Varian Gemini 200 MHz NMR or a Varian Unity 400 MHz NMR; chemical shift values were internally referenced to TMS, or to the residual proton signals of the solvent (δ, C*H*Cl_3). Infrared spectra (Nujol mulls, KBr optics) were recorded on a Nicolet 20SX/C FTIR spectrometer at 2 cm^{-1} resolution. UV−visible spectra of $(CN)_2T_n$ ($n = 2-6$) were recorded (in DMSO) on a Perkin-Elmer Lambda 6 spectrophotometer. Mass spectra (70 eV, EI) were obtained on a Kratos MS890 spectrometer. Elemental analyses were performed by MHW Laboratories, Phoenix, AZ.

Synthesis of 2,2′:5′,2″:5″,2‴-Quaterthiophene. This compound has been prepared previously[27b] by a different route.

(48) Philogène, B. J. R.; Arnason, J. T.; Berg, C. W.; Duval, F.; Champagne, D.; Taylor, R. G.; Leitch, L. C.; Morand, P. *J. Econ. Entom.* **1985**, *78*, 121.

Under an atmosphere of nitrogen 2-bromothiophene (17.0 g, 100 mmol) in 50 mL of diethyl ether was added to a slurry of magnesium (3.00 g, 0.123 mol) in ether. The reaction was initiated with a small amount of the bromo solution and a crystal of iodine. Once the vigorous reaction had started, the rest of the bromo solution was added dropwise to the ice-cooled magnesium slurry over the course of 20 m. This solution was allowed to warm to room temperature and stirred for an additional 2 h before being cannulated into an ice-cooled solution of dibromobithiophene (Br_2T_2, 13.6 g, 42.0 mmol) and the coupling reagent Ni(dppp)Cl_2 (0.46 g, 0.85 mmol). The following day the reaction mixture was poured onto 500 mL of saturated NH_4Cl solution, and the precipitate filtered off to yield of 11.7 g (35.5 mmol) of quaterthiophene H_2T_4 (84%). The crude material was recrystallized from chlorobenzene.

Preparation of 2,2′:5′,2″:5″,2‴:5‴,2⁗:5⁗-Quinquethiophene. An alternate synthesis is given to the previously reported route.[49] As above, a Grignard reagent was generated in situ from 2-bromothiophene (12.3 g, 75.0 mmol) in 30 mL of ether and magnesium (2.70 g, 0.111 mol) in 10 mL of ether. This mixture was then cannulated into a solution of 5,5″-dibromo-2,2′:5′,2″-terthiophene (Br_2T_3, 12.3 g, 30.0 mmol) and Ni(dppp)-Cl_2 (0.30 g, 0.55 mmol) in 250 mL of ether and 200 mL of toluene. Workup as above and recystallization from chlorobenzene gave 10.4 g (25.2 mmol) of quinquethiophene (H_2T_5, 83%).

Preparation of 5,5⁗-Dibromo-2,2′:5′,2″:5″,2‴:5‴,2⁗:5⁗-quinquethiophene. This compound has been reported but not fully characterized.[50] Quinquethiophene H_2T_5 (2.0 g, 4.8 mmol) was slurried in 350 mL of DMF at 70 °C. A solution of NBS (1.73 g, 9.70 mmol) in DMF (50 mL) was added dropwise over 15 min. This solution was left stirring for 2 h before being poured onto 500 mL of crushed ice. The crude product was filtered and recrystallized from chlorobenzene to give 2.17 g (3.82 mmol) of golden dichromic flakes of Br_2T_5 (75%), mp 283−285 °C (lit. mp 289−291 °C[50]). Infrared spectrum (2000−400 cm^{-1}): 1071 (w), 971 (w), 840 (m), 830 (w), 794 (s), 698 (w), 458 (m) cm^{-1}. Mass spectrum: 570 (M^+, 100%), 492 ([M − Br]$^+$, 70%), 447 ([M − CSHBr]$^+$, 15%), 412 ([M − 2Br]$^+$, 11%), 367 ($C_{19}H_{11}S_4^+$, 12%), 285 ($C_{15}H_9S_3^+$, 14%), 233 (21%), 98 (21%). Anal. Calcd for $C_{20}H_{10}Br_2S_5$: C, 42.11; H, 1.77; Br, 28.02%. Found: C, 42.08; H, 1.83; Br, 28.24%.

Preparation of 2,2′:5′,2″-Terthiophene-5-carbonitrile. This compound (which is a natural product) has been prepared previously by another route.[51] Bromoterthiophene (HT_3Br, 7.00 g, 21.4 mmol) and copper(I) cyanide (2.50 g, 28.0 mmol) was refluxed in 70 mL of quinoline for 2 h. The resultant mixture was poured on 300 mL of crushed ice with 70 mL of concentrated HCl. The crude product was filtered, washed copiously with water and ethanol, and air-dried. It was purified by sublimation in vacuo at 120 °C to give 4.72 g (17.3 mmol) of yellow blocks of HT_3CN (81%), mp 124−125 °C (lit. mp 104−105 °C[51]). This material was recrystallized from ethanol prior to further use. ^{1}H NMR (δ, $CDCl_3$): 7.51 (d, 1H), 7.26 (d, 1H), 7.20 (dd, 1H), 7.17 (s, 1H), 7.10 (d, 1H), 7.03 (AB, 2H). ^{13}C NMR (δ, $CDCl_3$, ^{1}H decoupled): 144.9, 139.6, 138.8, 136.8, 133.8, 128.6, 127.2, 125.9, 125.0, 123.7, 114.6. Infrared spectrum (2500−400 cm^{-1}): 2216 (s), 1421 (w), 1336 (w), 1254 (w), 1224 (w), 1204 (w), 1195 (w), 1157 (w), 1065 (w), 1049 (m), 870 (w), 841 (m), 797 (s), 702 (m), 550 (w), 526 (w), 480 (w) cm^{-1}. Mass spectrum: *m/e* 273 (M^+, 100%), 248 ([M − CN]$^+$, 9%), 228 (4%), 203 ($C_{11}H_7S_2^+$, 3%).

Preparation of 5-Bromo-2,2′:5′,2″-terthiophene-5″-carbonitrile. Terthiophenecarbonitrile HT_3CN (3.73 g, 13.7 mmol) was dissolved in 40 mL of DMF. NBS (2.44 g, 13.7 mmol) was added portionwise over 20 min. Precipitation of product occurs upon addition of about 25% of the NBS. This solution was stirred for 2 h, then poured into 200 mL of water, and suction filtered. The crude material was recrystallized from 450 mL of CH_3CN to yield BrT_3CN (4.30 g, 12.2 mmol, 89%), mp 152−154 °C. Before using this material in further reactions, it was purified by sublimation in vacuo at 140 °C and recrystallized a second time to give yellow needles. ^{1}H NMR (δ, $CDCl_3$): 7.51 (d, 1H), 7.16 (d, 1H), 7.10 (d, 1H), 7.03 (d, 1H), 6.96 (AB, 2H). Infrared spectrum (2500−400 cm^{-1}): 2116 (s), 1414 (w), 1341 (w), 1216 (m, br), 1043 (m), 1171 (w), 1150 (w), 973 (w), 900 (w), 865 (w), 789 (s), 737 (w, br), 688 (w), 654 (w), 539 (m), 511 (w), 473 (m) cm^{-1}. Mass spectrum: *m/e* 353 (M^+, 100%), 272 ([M − Br]$^+$, 15%), 228 ([M − CSHBr]$^+$, 48%), 69 (14%). Anal. Calcd for $C_{13}H_6BrNS_3$: C, 44.32; H, 1.72; N, 3.98%. Found: C, 44.27; H, 1.91; N, 4.00%.

General Synthetic Method for the Conversion of Dibromooligothiophenes to Oligothiophenedicarbonitriles. The dibromo compound was slurried in quinoline with a 40% molar excess of CuCN, and the mixture heated at reflux for 2−3 h. After this time, the reaction mixture was cooled and quenched by pouring it onto a mixture of ice and concentrated HCl (the volume of HCl equal to the volume of quinoline). The dark precipitate was filtered, washed copiously with water and ethanol, and dried in air for several hours. The crude material was taken up in an excess of chlorobenzene and hot filtered, and the solution allowed to cool to room temperature. The powdery precipitate so obtained was filtered, washed with chlorobenzene, and air-dried. Purification for chemical analysis and X-ray work was effected by fractional vacuum sublimation.

Preparation of 2,2′:5′,2″-Terthiophene-5,5″-dicarbonitrile. This compound has been synthesized previously with a different route.[51] Dibromoterthiophene (Br_2T_3, 12.0 g, 30.0 mmol) in 100 mL of quinoline was converted to 6.5 g (21.8 mmol, 74%) of crude product that was purified by fractional sublimation at 160−110 °C/10^{-3} Torr to give yellow crystals of $(CN)_2T_3$, mp 204−205 °C (lit. mp of this compound contaminated with up to 30% monocyano derivative HT_3CN has been reported as 165−170 °C[51]). ^{1}H NMR (δ, $CDCl_3$): 7.54 (d, 2H), 7.22 (s, 2H), 7.15 (d, 2H). ^{13}C NMR (δ, $CDCl_3$, ^{1}H decoupled): 143.2, 138.3, 135.9, 126.8, 124.1, 113.8, 108.4. Infrared spectrum (2500−400 cm^{-1}): 2214 (s), 1438 (m), 1153 (w), 1044 (m), 864 (m), 813 (m), 788 (s), 725 (w, br), 554 (s), 506 (s) cm^{-1}. UV−vis (DMSO): λ_{max} 391 nm (ϵ 24 200 M^{-1} cm^{-1}). Mass spectrum: *m/e* 298 (M^+, 100%), 228 (5%), 154 (16%). Anal. Calcd for $C_{14}H_6N_2S_3$: C, 56.35; H, 2.03; N, 9.39%. Found: C, 56.31; H, 2.19; N, 9.31%.

Preparation of 2,2′:5′,2″:5″,2‴-Quaterthiophene-5,5‴-dicarbonitrile. Dibromoquaterthiophene (Br_2T_4, 5.00 g, 10.2 mmol) in 60 mL of quinoline was converted to 2.30 g (47.9 mmol, 59%) of crude product that was purified by fractional sublimation at 180−130 °C/10^{-3} Torr to give dark orange-red dichromic blocks of $(CN)_2T_4$, mp 279−280 °C. Infrared spectrum (2500−400 cm^{-1}): 2213 (s), 1542 (m), 1473 (w), 1438 (s), 1279 (m), 1216 (w), 1202 (w), 1161 (m), 1050 (s), 907 (w), 855 (s), 803 (s), 730 (w, br), 643 (w), 591 (w), 560 (w), 549 (m), 536 (w), 501 (m) cm^{-1}. UV−vis (DMSO): λ_{max} 423 nm (ϵ 42 400 M^{-1} cm^{-1}). Mass spectrum: *m/e* 380 (M^+, 10%), 355 ([M − CN]$^+$, 92%), 310 ($C_{16}H_8NS_3^+$, 46%), 216 ($C_{11}H_6NS_2^+$, 32%), 141 (59%), 112 (100%), 46 (H_2CS^+, 56%). Anal. Calcd for $C_{18}H_8N_nS_4$: C, 56.82; H, 2.12; N, 7.36%. Found: C, 56.86; N, 2.13; N, 7.46%.

Preparation of 2,2′:5′,2″:5″,2‴:5‴,2⁗:5⁗-Quinquethiophene-5,5⁗-dicarbonitrile. Dibromoquinquethiophene (Br_2T_5, 2.0 g, 3.5 mmol) in 30 mL of quinoline was converted to 1.02 g (1.82 mmol, 64%) of crude product that was purified by fractional sublimation at 220−180 °C/10^{-4} Torr to give bright red blocks of $(CN)_2T_5$, mp 258−260 °C. Infrared spectrum (2500−400 cm^{-1}): 2220 (m), 1154 (w, br), 1070 (m), 1046 (m), 920 (w, br), 890 (w), 848 (m), 837 (m), 796 (s, br), 726 (s), 560 (m), 539 (s), 501 (w), 487 (s), 466 (m), 435 (m). UV−vis (DMSO): λ_{max} 442 nm (ϵ 50 500 M^{-1} cm^{-1}). Mass spectrum: *m/e* 462 (M^+, 3%), 437 ([M − CN]$^+$, 100%), 412 (69%), 218 (14%). Anal. Calcd for $C_{22}H_{10}N_2S_5$: C, 57.12; H, 2.18; N, 6.06%. Found: C, 57.26; H, 2.40; N, 5.89%.

Preparation of 2,2′:5′,2″:5″,2‴:5‴,2⁗:5⁗,2‴′:5‴′-Sexithiophene-5,5‴′-dicarbonitrile. Nickel dichloride (78 mg, 0.62 mmol), powdered zinc (1.25 g, 19.0 mmol), and triphenylphosphine (1.25 g, 4.8 mmol) were subjected to several pump/refill with nitrogen cycles, then added to 20 mL of rigorously dried DMF (three times over fresh Linde 4 Å molecular sieves) at 65 °C to generate the Ni^0 coupling catalyst

(49) Nakayama, J.; Nakamura, Y.; Murabayashi, S.; Hoshino, M. *Heterocycles* **1987**, *26*, 939.

Table 8. Crystal Data

compound	$(CN)_2T_3$	$(CN)_2T_4$	$(CN)_2T_5$	$(CN)_2T_6$
formula	$S_3C_{14}N_2H_6$	$S_4N_2C_{18}H_8$	$S_5C_{22}N_2H_{10}$	$S_6C_{26}N_2H_{12}$
a, Å	18.363(7)	7.3254(9)	13.633(4)	13.8962(14)
b, Å	11.8356(9)	7.8658(6)	11.706(5)	5.9100(16)
c, Å	30.666(4)	8.1813(8)	37.073(8)	14.0798(16)
α, deg		64.706(8)		
β, deg	102.15(2)	76.059(8)	90.22(2)	98.446(4)
γ, deg		76.692(8)		
V, Å^3	6515(3)	409.29(7)	5929(3)	1143.8(4)
d(calcd), g cm^{-3}	1.52	1.544	1.52	1.58
space group	*C*2/*c*	$P\bar{1}$	*C*2/*c*	$P2_1/a$
Z	20	1	12	2
data with $I > 3.0\sigma(I)$	1743	1177	2498	1172
$R(F)$, $R_w(F)$[a]	0.047, 0.070	0.031, 0.056	0.042, 0.061	0.038, 0.057

[a] $R = [\sum||F_o| - |F_c||]/[\sum|F_o|]$; $R_w = \{[\sum w||F_o| - |F_c||^2]/[\sum(w|F_o|^2)]\}^{1/2}$.

described previously.[28] Once the bright red catalyst had been generated, bromocyanoterthiophene (BrT_3CN, 1.0 g, 2.8 mmol) was added, and the solution stirred for 4 h. The solution was filtered and washed with boiling ethanol, then boiling water, and then acetone. The solid residue was taken up into boiling benzonitrile, and the mixture hot filtered to remove the residual zinc. Red platelets (412 mg, 0.640 mmol, 46%) of the dinitrile $(CN)_2T_6$ formed on cooling. This material was sublimed over a temperature gradient of 270−230 °C/10^{-4} Torr to give dark red crystals (0.26 g), mp 309−310 °C. Infrared spectrum (2500−400 cm^{-1}): 2220 (m), 1751 (w), 1591 (w), 1556 (w), 1522 (w), 1494 (m), 1439 (s), 1317 (w), 1272 (w), 1160 (w), 1074 (m), 1046 (m, br), 879 (w), 844 (s), 827 (s), 790 (s), 563 (w), 549 (s), 529 (s), 504 (m), 483 (s) cm^{-1}. UV−vis (DMSO): λ_{max} 461 nm.[52] Mass spectrum: *m*/*e* 544 (M^+, 100%), 519 ([HM − CN]$^+$, 4%), 437 ([HM − C_4H_2SCN]$^+$, 8%), 272 ([$(C_4H_2S)_3CN$]$^+$, 17%). Anal. Calcd for $C_{26}H_{12}N_2S_6$: C, 57.33; H, 2.22; N, 5.14%. Found: C, 57.59; H, 2.38; N, 4.89%.

X-ray Measurements. All X-ray data were collected on an Enraf-Nonius CAD-4 diffractometer with monochromated Mo Kα radiation ($\lambda = 0.7107$ Å). Crystals were mounted on a glass fiber with silicone. Data were collected using a $\theta/2\theta$ technique. The structures were solved using direct methods and refined by full-matrix least squares which minimized $\sum w(\Delta F)^2$. A summary of crystallographic data is provided in Table 8.

Electronic Structure Calculations. All calculations were performed on a Pentium 166 PC. The MNDO calculations were carried out using the MOPAC93 suite of programs[53] (compiled to run under DOS). Calculations on H_2T_n and $(CN)_2T_n$ ($n = 2-6$) were performed with full geometry optimization within the constraints of C_{2h} (*n* even) and C_{2v} (*n* odd) symmetry, i.e., all-trans geometries. The band structure calculations were carried out on a Pentium 166 PC with the EHMACC suite of programs[54] (compiled to run under DOS) using the parameters discussed previously.[55] The off-diagonal elements of the Hamiltonian matrix were calculated with the standard weighting formula.[56,57] Atomic coordinates were taken from the X-ray data.

Acknowledgment. We thank the Natural Sciences and Engineering Research Council of Canada, the NSF/EPSCOR program and the State of Arkansas for financial support. We also acknowledge NSERC for a postgraduate scholarship (to C.D.M.) and the Department of Education for a doctoral fellowship (to T.M.B.).

Supporting Information Available: Tables of crystal data, structure solution and refinement, bond lengths and angles, torsion angles, intermolecular contacts, and anisotropic thermal parameters for the structures reported (21 pages). This material is contained in many libraries on microfiche, immediately follows this article in the microfiche version of the journal, and can be downloaded from the Internet; see any current masthead page for ordering information and Internet access instructions.

CM960545L

(50) Luo, T.-m. H.; LeGoff, E. *J. Chin. Chem. Soc. (Taipei)* **1992**, *39*, 325.
(51) Soucy-Breau, C.; MacEachern, A.; Leitch, L. C.; Arnason, T.; Morand, P. *J. Heterocycl. Chem.* **1991**, *28*, 411.
(52) The extinction coefficient for this compound could not be measured accurately because of its extremely low solubility. The spectrum was recorded from a saturated solution in DMSO.
(53) MOPAC93, Quantum Chemistry Program Exchange.
(54) EHMACC, Quantum Chemistry Program Exchange.
(55) Basch, H.; Viste, A.; Gray, H. B. *Theor. Chim. Acta* **1965**, *3*, 458.
(56) Ammeter, J. H.; Burghi, H. B.; Thibeault, J. C.; Hoffmann, R. *J. Am. Chem. Soc.* **1978**, *100*, 3686.
(57) Cordes, A. W.; Haddon, R. C.; Oakley, R. T.; Schneemeyer, L. F.; Waszczak, J. V.; Young, K. M.; Zimmerman, N. M. *J. Am. Chem. Soc.* **1991**, *113*, 582.